



Title	Smallest ( ~ 10nm) phase-change marks in amorphous and crystalline Ge <sub>2</sub> Sb <sub>2</sub> Te <sub>5</sub> films
Author(s)	Tanaka, Keiji
Citation	Journal of Non-Crystalline Solids, 353(18-21), 1899-1903 <a href="https://doi.org/10.1016/j.jnoncrysol.2007.02.020">https://doi.org/10.1016/j.jnoncrysol.2007.02.020</a>
Issue Date	2007-06-15
Doc URL	<a href="http://hdl.handle.net/2115/28127">http://hdl.handle.net/2115/28127</a>
Type	article (author version)
File Information	JNCS353-18-21.pdf



[Instructions for use](#)

# **SMALLEST (~10 nm) PHASE-CHANGE MARKS IN AMORPHOUS AND CRYSTALLINE Ge<sub>2</sub>Sb<sub>2</sub>Te<sub>5</sub> FILMS**

**Keiji Tanaka**

Department of Applied Physics, Graduate School of Engineering, Hokkaido University,  
Sapporo 060-8628, Japan ([keiji@eng.hokudai.ac.jp](mailto:keiji@eng.hokudai.ac.jp))

Electrical nano-scale crystallization and amorphization in amorphous and crystalline Ge<sub>2</sub>Sb<sub>2</sub>Te<sub>5</sub> films have been studied using scanning probe microscopes. In scanning tunneling microscopes, the phase changes can be induced, not by tunneling currents, but by conducting currents flowing through contacted probes. In an atomic force microscope, metallic cantilevers can produce phase-change marks with minimal sizes of ~10 nm. The crystallization and amorphization processes show different dependences upon thickness of Ge<sub>2</sub>Sb<sub>2</sub>Te<sub>5</sub> films. These features are discussed from thermo-dynamical and microscopic structural points-of-view.

PACS codes: 81.05.Gc, 81.07.-b, 73.61.Jc, 65.60.+a

## 1. Introduction

The phase-change recording has markedly progressed in this decade, and its ultimate characteristics lend considerable interest. Among those, the memory capacity is one of the most important, which is determined in principle by a mark size. In optical phase-change systems such as DVD-RAM, the size is greater than  $\sim 100$  nm in diameter, which is governed by diffraction or evanescent-wave characters of laser light [1,2]. Nevertheless, recording materials, e.g.  $\text{Ge}_2\text{Sb}_2\text{Te}_5$  films, appear to have capabilities of storing much smaller marks. Actually, several studies have demonstrated such possibilities using electrical phase changes [3-6], in which the mark size can be reduced using small electrodes. (Note that the mechanisms of optical and electrical phase changes are both thermal; i.e. laser and Joule heating.) However, most of previous studies deal with amorphous-to-crystalline ( $a \rightarrow c$ ) phase changes, and the reverse  $c \rightarrow a$  change has been little investigated. This is because the amorphization can occur after melting at  $\sim 600^\circ\text{C}$ , which is much higher than the crystallization temperature of  $\sim 170^\circ\text{C}$  [7]. It is therefore valuable to examine formation characteristics of crystalline and amorphous nano-scale marks in amorphous ( $a$ -) and crystalline ( $c$ -) Ge-Sb-Te films, respectively, under comparable experimental conditions.

In the present work, we will study electrical  $a \rightarrow c$  and  $c \rightarrow a$  phase changes from a unified viewpoint. At the outset, the experimental results obtained for single  $\text{Ge}_2\text{Sb}_2\text{Te}_5$  films using a scanning tunneling microscope (STM) [8,9] and an atomic force microscope (AFM) [9,10] are briefly summarized, which have been published separately (see, also reviews [11,12]). We then compare several characteristics, including mark sizes and threshold powers of the phase changes. We also compare these experimental results with recent calculations reported by Wright et al. [13].

## 2. Experiments

$\text{Ge}_2\text{Sb}_2\text{Te}_5$  films with thicknesses of 1–900 nm were dc sputtered onto substrates such as glass slides which had been coated by thin films of Au-Ni (20nm-thick) or Pt (50nm-thick), which worked as bottom electrodes. Sputtered films were amorphous, and these were employed for inspecting  $a \rightarrow c$  changes. In addition, the films were crystallized to the cubic phase by heat treatment at  $200^\circ\text{C}$  for investigating  $c \rightarrow a$  changes. Crystallite size in the annealed films was estimated at  $\sim 10$  nm using x-ray diffraction. Electronic properties of these films were evaluated previously [7], the results being consistent with others [14,15]. Surface roughness of films, e.g., with thickness of 100 nm was smaller than  $\sim 5$  nm, which was important to production of nano-scale marks. It should be mentioned here that the crystalline films were more susceptible to oxidize, and accordingly, phase-change experiments were performed immediately ( $< 5$  h) after sample preparations. Phase-change marks were produced and imaged using an AFM (SPA300, Seiko Instruments) and STMs (Nanoscope E, DI and SPA300, Seiko Instruments), through which voltage pulses with durations of 3 ns – 10 ms were applied. The AFM was equipped with  $\text{Si}_3\text{N}_4$  cantilevers (Veeco, DNP-S), which were coated with Au-Ni, and homemade Au probes. On the other hand, STM probes were homemade from W wires. Structural changes were inspected using micro-Raman and x-ray

diffraction systems.

### 3. Results

#### 3.1. Comparison of STM and AFM characteristics

Before experiments, we had expected that an STM could produce smaller marks, because in general it can provide atomic images with less difficulty [16]. However, observations were opposite; e.g., minimal crystalline marks produced in a-Ge<sub>2</sub>Sb<sub>2</sub>Te<sub>5</sub> being ~50 nm for the STM [8] and ~10 nm for the AFM [10]. This is because the tunneling current, which is practically limited to be smaller than ~100 pA for Ge<sub>2</sub>Sb<sub>2</sub>Te<sub>5</sub> films, cannot provide sufficient Joule heats needed for phase changes. In the STM, phase-change marks can be produced by conducting currents (~3 V, ~1 mA, and ~10 ns) flowing through an inserted W tip, which has been electrically-elongated by applied pulse voltages [8,11,12]. The inserted tip gives concave (M-shaped) deformations on film surfaces and uncontrollable electrical powers, and accordingly, the mark becomes necessarily greater. Note that this idea, i.e., the phase change in the STM occurs after tip contacting, is consistent with similar dependences of mark size and threshold power (or voltage) in the AFM and STM phase changes on film thickness [9-11]. Therefore, for producing smaller marks, the AFM is more useful at present. It should be mentioned, however, that a possibility of producing small amorphous marks using STMs remains by shortening applied pulses to ~1 ns, which is a time scale of tip elongation [9].

On the other hand, reproducibility of mark formation by the STM is better than that by the AFM. Actually, an STM tip could produce more than 25 marks (Fig. 1), but the AFM had difficulties in producing 10 marks. This reproducibility difference arises from two reasons. One is differences in elastic and thermal properties of the probe materials; Au(:Ni) for the AFM and W for the STM. The AFM cantilever must be flexible for possessing small spring constants [16], which makes the cantilever inevitably fragile. In addition, an Au(:Ni)-probe apex tends to soften upon intense Joule heating. The other is, in the present AFM, the probe always scratches film surfaces, which is likely to destroy the apex and enlarge the curvature, which causes larger marks. It should be mentioned here that, by scanning tips with dc voltages, the STM can provide electrochemical nano-lithography [17].

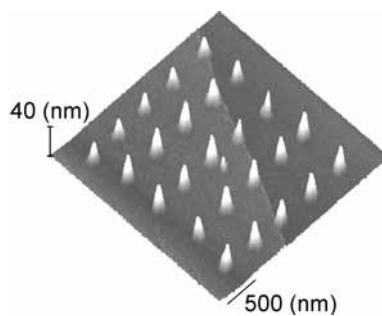


Fig. 1. Arrayed amorphous marks produced in a 150nm-thick c-Ge<sub>2</sub>Sb<sub>2</sub>Te<sub>5</sub> film by applying pulses with 10 V and 100  $\mu$ s (nominal duration [8]) using the STM.

### 3.2. Comparison of a→c and c→a changes

Since the AFM is more appropriate to produce nano-scale marks, as described in 3.1, we focus on its feature hereafter [9-11]. It should be mentioned first that the a→c and c→a phase changes have occurred irrespective of the polarity of applied voltages, which is consistent with an idea that the crystallization and amorphization are induced by Joule heats.

Interestingly, minimal marks produced in a→c and c→a are nearly the same in size. The smallest crystalline mark obtained in a 1nm-thick a-Ge<sub>2</sub>Sb<sub>2</sub>Te<sub>5</sub> film appears to be facet-like with a diameter of ~10 nm [10], and the smallest amorphous mark obtained in a 250nm-thick c-Ge<sub>2</sub>Sb<sub>2</sub>Te<sub>5</sub> film is a mound type with a diameter of ~10 nm [9]. However, it has been difficult to produce such small marks in reproducible way, and produced marks tend to disappear within one day. Needed energies have been appreciably different. For instance, for producing the smallest marks, the crystallization needs ~100 pJ (0.6 mW and 200 ns pulse) and the amorphization needs 30 pJ (~1.5 mW and 20 ns pulse). Note that these energies are contrastive to the relevant temperatures for the a→c and c→a processes, which are the crystallization temperature (~170°C) and the melting temperature (~600°C). Produced marks can be erased, while the reproducibility remains to be improved.

Dependences of the two processes upon the film thickness are markedly different as shown in Fig. 2. In the a→c process, the mark size and the threshold voltage tend to increase with the film thickness [10]. In thinner films than ~5 nm, however, the minimal size remains at ~10 nm. In contrast, in the c→a, the mark size and the threshold energy decrease with the film thickness at 20–100 nm and these become mostly independent at 100–500 nm [9].

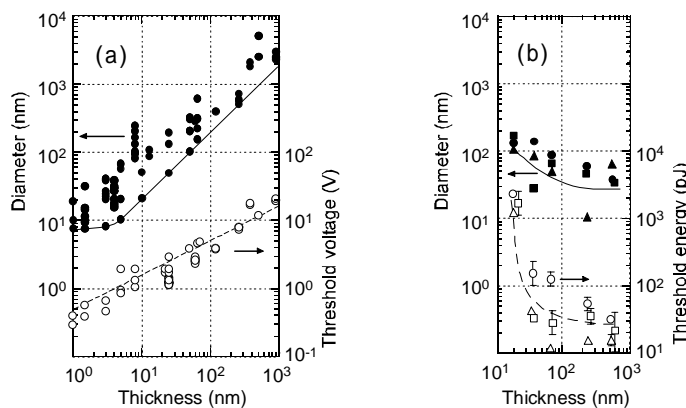


Fig. 2. Dependences of mark diameter and threshold voltage (energy) upon the film thickness in (a) a→c and (b) c→a changes using the AFM.

Dependences of the mark diameter on pulse duration  $\tau$  are common in the a→c and c→a changes. The diameter increases in proportion to  $\tau^{1/2}$  at  $\tau = 20$  ns-1 ms for crystallization [10,11] and at  $\tau = 5\sim 100$  ns for amorphization [9].

Transient characteristics of the a→c and c→a changes are contrastive as shown in Fig. 3. In the a→c change, after some incubation time, suddenly the voltage drops and the current increases. On the other hand, in the c→a changes, the resistance continuously decreases. Here,

we should note the following important difference: The  $a \rightarrow c$  phase change is assumed to occur within pulse intervals [18]. In the  $c \rightarrow a$  changes, however, a crystalline film is just melted by an electrical pulse, and after termination of the pulse, the melt will be quenched into an amorphous state. The quenching process is difficult to probe electrically.

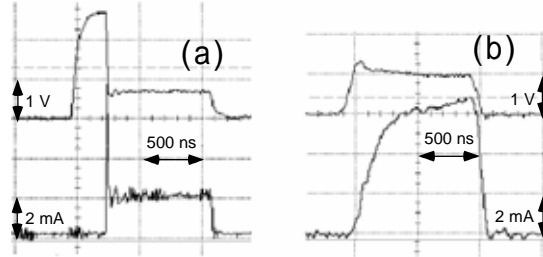


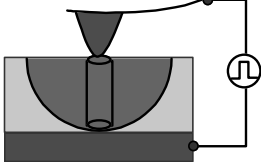
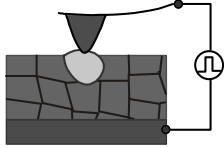
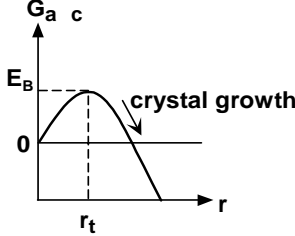
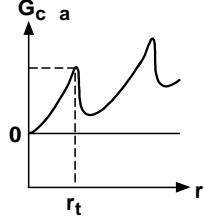
Fig. 3. Typical transient characteristics of the (a)  $a \rightarrow c$  and (b)  $c \rightarrow a$  changes in amorphous and crystalline films with thickness of 250 nm. Voltage pulses are applied through load resistances of 1 k $\Omega$  in the  $a \rightarrow c$  and 50  $\Omega$  in the  $c \rightarrow a$ .

#### 4. Discussion

It is known that the crystallization and amorphization occur through different processes. Electrically,  $a\text{-Ge}_2\text{Sb}_2\text{Te}_5$  is nearly insulating ( $\sim 10^4$   $\Omega\text{cm}$  [7]) at room temperature, and a voltage pulse first produces an electrical conducting channel [18]. The transient can be inferred from current changes, while the mechanism of channel formation remains controversial [18,19]. Once the channel being formed, a higher current provides Joule heat, giving rise to a substantial temperature rise, and the crystallization takes place. On the other hand, a crystalline film is much more conducting ( $\sim 10^0$   $\Omega\text{cm}$  [7]), so that electrical inputs can directly heat the film to melting. These two electro-thermal processes cause the  $a \rightarrow c$  and  $c \rightarrow a$  phase changes.

Taking these insights into account, we assume contrastive phase growths, as summarized in Table 1. In the crystallization, after (or simultaneously with) the channel formation, the crystallization starts at (or near) the probe-film contact, which proceeds as an exothermic reaction at  $\sim 170^\circ\text{C}$ . However, if the input electrical power is critical, when the crystalline front reaches the bottom electrode, the growth will stop due to large heat dissipation to the metallic electrode and so forth. Accordingly, the size of minimal crystalline marks is proportional to the film thickness as shown in Fig. 2. On the other hand, a melting in the amorphization process can start also at the probe-film contact, reflecting hemi-spherically spreading electric fields from the contact. In addition, since the melting needs latent heats, its growth tends to cease spontaneously, which is consistent with calculated temperature distributions [13]. Then, after quenching, only a surface layer can be transformed to an amorphous state. Note that the film thickness has no effect in this interpretation, which is consistent with the observations. Or, more precisely, thicker films are more likely to be heated due to small thermal conductivities of  $\text{Ge}_2\text{Sb}_2\text{Te}_5$  films [20], which is consistent with the decrease in the threshold energy with the thickness in the  $c \rightarrow a$  process (Fig. 2).

Table 1 Comparison of  $a \rightarrow c$  and  $c \rightarrow a$  phase changes.

phase change	$a \rightarrow c$		$c \rightarrow a$
process	channel formation	heating	direct heating
related temperature	crystallization ( $\sim 170^\circ\text{C}$ )		melting ( $\sim 600^\circ\text{C}$ )
thermal reaction	exothermic		endothermic
model			
energy change	$\Delta G_c + \Delta G_{ac}$		$\Delta G_a + \Delta G_{ac} - \Delta G_{cc}$
			

Why are the minimal mark sizes produced in the  $a \rightarrow c$  and  $c \rightarrow a$  processes by the AFM commonly  $\sim 10$  nm ? It may be plausible that the size is governed by transient behaviors of a cantilever apex, which penetrates into the semi-conducting films when subjected to pulsed voltages [21,22]. However, quantitative evaluation of this process is difficult.

Otherwise, this coincidence is subtle, which can be understood on thermodynamic and structural ideas as follows (see Table 1): The free-energy change  $\Delta G_{a \rightarrow c}$  for crystallization in amorphous films can be written as  $\Delta G_{a \rightarrow c} = \Delta G_c + \Delta G_{ac}$ , where  $\Delta G_c$  ( $< 0$ ) is a free-energy stabilization with crystallization and  $\Delta G_{ac}$  ( $> 0$ ) is an interfacial energy. Provided that the mark is spherical with a radius  $r$ ,  $\Delta G_c$  and  $\Delta G_{ac}$  are proportional to  $-r^3$  and  $+r^2$ . Accordingly,  $\Delta G_{a \rightarrow c}$  can have a barrier (higher than  $\sim 30$  meV, which is thermal energy at crystallization temperature) at a certain  $r_c$ , which appears to be 5-10 nm, when putting plausible values [11,12]. This radius is consistent with the size ( $\sim 10$  nm) of minimal crystalline marks. It should be mentioned that this scale is also comparable to reported sizes of crystalline grains produced optically [23] and thermally [24], which may lend supports to this rough idea.

However, a simple extension of this model to the  $c \rightarrow a$  change,  $\Delta G_{c \rightarrow a} = \Delta G_a + \Delta G_{ac}$ ,

cannot be accepted. Because the free-energy change  $\Delta G_a$  for amorphization in crystalline films is positive, and no energy minima appear. Then, we modify the equation as  $\Delta G_{c \rightarrow a} = \Delta G_a + \Delta G_{ac} - \Delta G_{cc}$ , where  $\Delta G_{cc} (>0)$  is the interfacial energy between crystalline clusters [9], assuming that a single crystallite, or its multiples, is converted to an amorphous cluster. Then, if  $\Delta G_{ac} < \Delta G_{cc}$ ,  $\Delta G_{c \rightarrow a}$  can have a minimum at the crystallite size, which has been estimated at  $\sim 10$  nm from the x-ray analysis as mentioned in 2. That is, in this interpretation, the size of amorphous marks is determined by the original crystallite size, which could not be modified experimentally [9]. This interpretation may be consistent with the dramatic increase in the threshold energy when the film thickness decreases to  $\sim 10$  nm (Fig. 2(b)). In short, the minimal sizes of amorphous and crystalline marks can be governed, respectively, by nucleation kinetics and crystallite sizes. Of course, applications of thermodynamic theories are limited at nano-scales, and more elaborate microscopic calculations are needed.

Finally, we note that the ultimate mark size of  $\sim 10$  nm suggests a possibility of producing phase-change memories having *tera-byte* capacities. The above model implies that this size of crystalline marks is the smallest limit obtained at room temperature, although at cryogenic temperatures an atomic memory ( $\sim 0.1$  nm) has been demonstrated by Eigler et al. [25].

## 5. Conclusions

Comparison of the  $a \rightarrow c$  and  $c \rightarrow a$  electrical phase changes using an STM and AFMs suggests that the AFM is more suitable for producing nano-scale marks. Minimal crystalline and amorphous marks obtained in  $\text{Ge}_2\text{Sb}_2\text{Te}_5$  films are  $\sim 10$  nm in diameter. Crystallization and amorphization characteristics show different dependences upon the film thickness, which can be ascribed to contrastive electrical conductivities of  $a$ - and  $c$ - $\text{Ge}_2\text{Sb}_2\text{Te}_5$  films and thermo-structural aspects of the phase changes.

## Acknowledgements

The author would like to thank his previous coworkers, Drs. T. Gotoh and K. Sugawara, and graduated students, H. Satoh and T. Kato.

## References

- [1] H. Tabata, K. Tokui, S. Higuchi, H. Moriizumi, and I. Matsumoto, Jpn. J. Appl. Phys. 45 (2006) 1204.
- [2] M. Shinoda, K. Saito, T. Ishimoto, T. Kondo, A. Nakaoki, N. Ide, M. Furuki, M. Takeda, Y. Akiyama, T. Shimouma, and M. Yamamoto, Jpn. J. Appl. Phys. 44 (2005) 3537.
- [3] T. Gotoh, K. Sugawara, and K. Tanaka, J. Non-Cryst. Solids 299-302 (2002) 968.
- [4] H. Tanaka, T. Nishihara, T. Ohtsuka, K. Morimoto, N. Yamada, and K. Morita, Jpn. J. Appl. Phys. 41 (2002) L1443.
- [5] S. Gidon, O. Lemonnier, B. Bichet, C. Dressler, and Y. Samson, Appl. Phys. Lett. 85 (2004) 6392.

- [6] H.F. Hamann, M. O'Boyle, Y.C. Martin, M. Rooks, and H.K. Wickramasinghe, *Nature Mater.* 5 (2006) 384.
- [7] T. Kato and K. Tanaka, *Jpn. J. Appl. Phys.* 44 (2005) 7340.
- [8] K. Sugawara, T. Gotoh, and K. Tanaka, *Jpn. J. Appl. Phys.* 43 (2004) L676.
- [9] H. Satoh, K. Sugawara, and K. Tanaka *J. Appl. Phys.* 99 (2006) 24306.
- [10] T. Gotoh, K. Sugawara, and K. Tanaka, *Jpn. J. Appl. Phys.* 43 (2004) L818.
- [11] K. Tanaka, T. Gotoh and K. Sugawara, *J. Optoelectron. Adv. Mater.* 6 (2004) 1133.
- [12] K. Sugawara, K. Tanaka, and T. Gotoh, *Oyo-Butsuri* 73 (2004) 910.
- [13] C.D. Wright, M. Armand, and M.M. Aziz, *IEEE Trans. Nanotechnol.* 5 (2006) 50.
- [14] B.-S. Lee, J.R. Abelson, S.G. Bishop, D.-H. Kang, B. Cheong, K.-G. Kim, *J. Appl. Phys.* 97 (2005) 93509.
- [15] S.A. Baily, D. Emin, H. Li, *Solid St. Commun.* 139 (2006) 161.
- [16] R. Wiesendanger, *J. Vac. Sci. Technol.* B12 (1994) 515.
- [17] K. Sugawara, T. Gotoh, and K. Tanaka, *J. Non-Cryst. Solids* 326&327 (2003) 37.
- [18] A. Madam and M.P. Shaw, *The Physics and Applications of Amorphous Semiconductors*, (Academic Press, Boston, 1988) Chap. 5.
- [19] P. Fantini, A. Pirovano, D. Ventrice, and A. Redaelli, *Appl. Phys. Lett.* 88 (2006) 263506.
- [20] C. Peng, L. Cheng, and M. Mansuripur, *J. Appl. Phys.* 82 (1997) 4183.
- [21] O. Schneegans, F. Houzé, R. Meyer, and L. Boyer, *IEEE Trans. Component, Packing, and Manufacturing Technol.* A21 (1998) 76.
- [22] G.M. Sacha, A. Verdaguer, J. Martinez, J.J. Sáenz, D.F. Ogletree, and M. Saimeron, *Appl. Phys. Lett.* 86 (2005) 123101.
- [23] M. Naito, M. Ishimaru, Y. Hirotsu, and M. Takashima, *J. Non-Cryst. Solids* 345&346 (2004) 112.
- [24] Y.J. Park, J.Y. Lee, M.S. Youm, and Y.T. Kim, *Jpn. J. Appl. Phys.* 44 (2005) 326.
- [25] D.M. Eigler and E.K. Schweizer, *Nature* 344 (1990) 524.